Published in final edited form as:
J Cell Physiol. 2009 January ; 218(1): 157–166. doi:10.1002/jcp.21581.

p38-MAPK- and Caspase-3-Mediated Superoxide-Induced Apoptosis of Rat Hepatic Stellate Cells: Reversal by Retinoic Acid

Noor Mohamed Jameel[1], **Chinnasamy Thirunavukkarasu**[1], **Tong Wu**[2], **Simon C. Watkins**[3], **Scott L. Friedman**[4], and **Chandrashekhar R. Gandhi**[1,2,5,*]

[1]Department of Surgery, Thomas E. Starzl Transplantation Institute, University of Pittsburgh, Pittsburgh, Pennsylvania

[2]Department of Pathology, University of Pittsburgh, Pittsburgh, Pennsylvania

[3]Department of Cell Biology, University of Pittsburgh, Pittsburgh, Pennsylvania

[4]Department of Medicine, Mount Sinai Medical Center, New York, New York

[5]VA Pittsburgh Healthcare System, Pittsburgh, Pennsylvania

Abstract

Reactive oxygen species (ROS) activate retinoid-containing quiescent hepatic stellate cells (qHSCs) to retinoid-deficient fibrogenic myofibroblast-like cells (aHSCs). However, ROS also cause apoptosis of aHSCs, and apoptotic aHSCs are observed in inflammatory fibrotic liver. Here, we investigated mechanisms of the effects of oxidative stress on the survival of qHSCs and aHSCs. HSCs from normal rat liver were used after overnight culture (qHSCs), or in 3–5 passages (aHSCs). For in vivo induction of oxidative stress, *tert*-butylhydroperoxide was injected into control and CCl4-induced cirrhotic rats. Spontaneous caspase-3 activation and apoptosis, observed in cultured qHSCs, decreased with time and were unaffected by superoxide. In contrast, superoxide caused caspase-3 and p38-MAPK activation, reduction in Bcl-xL expression, and apoptosis in aHSCs. Inhibition of caspase-3 and p38-MAPK did not affect the viability of qHSCs in the absence or presence of superoxide, but inhibited superoxide-induced death of aHSCs. Glutathione (GSH) level and activities of superoxide dismutase (SOD), catalase and glutathione peroxidase (GPx) were lower in aHSCs than qHSCs. Superoxide increased GSH content, and activities of SOD, catalase and GPx in qHSCs but not in aHSCs. Incubation of *13-cis*-retinoic acid (RA)-treated aHSCs with superoxide increased their GSH content significantly, and prevented superoxide-induced p38-MAPK and caspase-3 activation while dramatically reducing the extent of apoptosis. Finally, oxidative stress induced in vivo caused apoptosis of aHSCs in cirrhotic but not of qHSCs in control rats. These results suggest that the absence of retinoids render aHSCs susceptible to superoxide-induced apoptosis via caspase-3 and p38-MAPK activation.

The quiescent hepatic stellate cells (qHSCs) maintain hepatic architecture and blood flow by producing components of extracellular matrix and contractility respectively. During liver injury, qHSCs lose stored retinoids and transform into proliferating, fibrogenic and highly contractile α-smooth muscle actin (α-SMA)-positive myofibroblast-like cells (activated HSCs; aHSCs), which play a major role in the pathophysiology of chronic liver disease (Geerts et al.,

*Correspondence to: Chandrashekhar R. Gandhi, Thomas E. Starzl Transplantation Institute, University of Pittsburgh, E-1518 BST, 200 Lothrop street, Pittsburgh, PA 15213. gandhics@upmc.edu.
Noor Mohamed Jameel and Chinnasamy Thirunavukkarasu contributed equally to this work.

1994; Friedman, 2000). Therefore, mechanisms of activation of qHSCs and strategies to eliminate aHSCs from the fibrotic liver are the topics of major interest.

Reactive oxygen species (ROS) are implicated in the initiation and progression of liver pathologies (Klebanoff, 1988; Pietrangelo, 1996). ROS cause DNA damage and death of several cell types including hepatocytes (Li et al., 1997, 1999; Rauen et al., 1997, 1999; Knight et al., 2002), but are also shown to stimulate proliferation of certain cells such as vascular smooth muscle cells (Li et al., 1997) and cardiac fibroblasts (Li et al., 1999). ROS-induced cellular lipid peroxidation and exogenous lipid peroxidation products were shown to stimulate activation, proliferation and collagen I synthesis in HSCs (Parola et al., 1993; Lee et al., 1995; Svegliati Baroni et al., 1998; Galli et al., 2005; Novo et al., 2006a). Activation of a small GTP-binding protein Rac1 was reported to be a mechanism of the oxidative stress-induced activation of HSCs both in vivo and in vitro (Choi et al., 2006). Furthermore, increased oxidative stress was reported to be a mechanism of TGF-α- and collagen I-induced activation and proliferation of HSCs (Lee et al., 1995). However, exogenous ROS and intracellular oxidative stress were also shown to cause apoptosis and/or necrosis of aHSCs and aHSC-like human portal myofibroblasts (Li et al., 2001; Kweon et al., 2003; Montiel-Duarte et al., 2004; Thirunavukkarasu et al., 2004a). Mechanisms underlying the contrasting effects of ROS on survival/proliferation of qHSCs and aHSCs are unclear. Therefore, we investigated DNA damage, viability, and various parameters associated with apoptosis to gain understanding of the mechanisms by which superoxide affects the survival of qHSCs and aHSCs. Additionally, effect of oxidative stress on HSCs, in vivo, in control and CCl_4-induced fibrotic liver was determined.

Experimental Procedures

Preparation of HSCs

The protocols were approved by the IACUC, University of Pittsburgh as per NIH regulations. HSCs, isolated from male Sprague–Dawley rats (450–500 g) and purified as described previously (Thirunavukkarasu et al., 2004a), were suspended in DMEM containing antibiotics and 10% fetal bovine serum/10% horse serum, plated at a density of 0.5×10^6 /cm^2, and used 24 h later (qHSCs) (Thirunavukkarasu et al., 2005). For full activation, HSCs were subcultured after 10–12 days in primary culture, and used between 3rd and 5th passages (aHSCs). All of the cells expressed α-SMA indicating activated phenotype (Geerts et al., 1994; Friedman, 2000).

Superoxide treatment and DNA damage by comet assay

The cells were incubated in serum-free medium containing 1 mM hypoxanthine (HX) or hypoxanthine and up to 2 mU/ml xanthine oxidase (XO). Higher concentration of XO caused rapid and progressive death of both HSC phenotypes. Medium containing detached cells was aspirated, and the attached cells were harvested using trypsin. The two fractions were pooled and centrifuged (1,100g/7min). The cell pellet was suspended in serum-free medium, centrifuged, mixed with 110 μl of 0.65% (w/v) low melting point agarose in PBS and placed onto frosted glass microscope slides coated with 140 μl of 1 % normal melting point agarose. Agarose was allowed to set for 10 min at 4°C, then cells were lysed for 24 h in 2.5 mM NaCl containing 100 mM Na_2 EDTA, 10 mM Tris and 10% DMSO. The slides were rinsed with water and electrophoresis buffer (300 mM NaOH, 1 mM EDTA, pH 13) and subjected to electrophoresis for 20 min (300 mA, 25 mV). The slides were washed with 0.4 M Tris–HCl, pH 7.5, rinsed with water then methanol, stained with ethidium bromide, and scored using an image analysis system attached to an upright fluorescence microscope (Olympus Provas AX 70) equipped with CY3-Rhodamine filter cube. The images were transported to a computer through a charge-coupled device camera (Metamorph, Universal Imaging Corporation,

Downingtown, PA). Tail length (migration of DNA away from the nucleus, μm), tail DNA (%) and tail moment (arbitrary units) were assessed as described (Helma and Uhl, 2000) in 50 cells each from replicate slides.

Viability and apoptotic signaling

Cell viability was determined by the MTT assay (Thirunavukkarasu et al., 2004a). To determine apoptosis, cells grown on glass coverslips were washed with ice-cold PBS, fixed in 2% paraformaldehyde (30 min), and washed. The cells were then stained with Hoechst-33342 (5 μg/ml) in PBS for 1 min, washed with water, and mounted in 50% glycerol containing 20 mM citric acid and 50 mM disodium orthophosphate. Apoptotic cells were identified by brightly stained condensed chromatin or nuclei by fluorescence microscopy (Eclipse E600, Nikon, Tokyo, Japan). Apoptosis was also confirmed by nick-end labeling of nuclear DNA. Briefly, 2% paraformaldehyde-fixed cells were washed with PBS and permeabilized with 0.1% triton X-100. After 3 washes with PBS, cells were incubated with 50 μl of TUNEL reaction mixture that included biotinylated dUTP (Roche Pharmaceuticals, Nutley, NJ) at 37°C for 1 h, washed with PBS (5×), and incubated with streptavidin CY3 (Jackson Laboratories, Bar Harbor, Maine) for 30 min. After washing, the TUNEL-positive nuclei were detected using BX51 Olympus fluorescent microscope.

For determination of apoptosis via flow cytometry, the medium containing detached cells was aspirated and the attached cells were harvested using trypsin. The two cell fractions were pooled, washed twice with PBS, and suspended in 10 mM HEPES, pH 7.4, containing 140 mM NaCl and 2.5 mM $CaCl_2$ (buffer A) at 1×10^6 cells/ml. Annexin-V_{cy3} (4 μg/ml) and 7-AAD (5 μg/ml) were added to 100 μ l of the suspension. After incubation at room temperature for 15 min in dark, buffer A (400 μl) was added, and flow cytometry was performed within 1 h.

Western blot analysis was performed to determine caspase-3 activation, and expression of Bax, Bcl2, and Bcl-xL, and caspase-3-like activity was measured using a caspase fluorescent assay kit (BD Biosciences-Clontech, San Jose, CA) as described previously (Thirunavukkarasu et al., 2004a).

GSH, SOD, catalase, and glutathione peroxidase (GPx)

Cells (2×10^6) were treated with 100 μl of 5% cold metaphosphoric acid for 10 min on ice, then scraped and centrifuged at 3,000g (10 min; 4°C). The supernatant was mixed with 800 μl of 200 mM potassium phosphate buffer (pH 7.8) containing 0.2 mM diethylene-triamine-pentaacetic acid and 0.025% LUBROL, and 50 μl of 12 mM chromogenic reagent in 0.2 NHCl (Glutathione Assay Kit, Calbiochem,San Diego, CA). The color developed after 10 min in dark at 25°C was read at 400 nm.

To assay enzyme activities, the cells were suspended in 0.1 M Tris–HCl, pH 7.4, ruptured by sonication, centrifuged (130 g; 10 min), and the supernatant was adjusted to 2 μg of protein/μl. For SOD assay, 100 μl of the supernatant was mixed with 125 μl of ethanol and 625 μl of chloroform in a mechanical shaker for 15 min and centrifuged. The supernatant (0.05 ml) was mixed with 0.1 ml of 0.1 M Tris–HCl, pH 8.2, 0.075 ml of distilled water and 0.025 ml of 1 mM pyrogallol in 0.05 M Tris–HCl, pH 7.4; absorbance was measured at 420 nm.

For catalase assay, 100 μl of the supernatant was mixed with 0.5 ml of 0.01 M phosphate buffer, pH 7.0, and 0.25 ml of 0.2 M H_2O_2. After 10 min at 37°C, 1.0 ml of diluted (1:5 in water) 5% dichromate-acetic acid (1:3; v/v) was added. H_2O_2 in the range of 0 to 20 μmol was treated similarly for comparison. The tubes were heated in a boiling water bath for 10 min; absorbance was measured 570 nm.

For GPx assay, 100 μl of the supernatant was mixed with 100 μl of 0.32 M phosphate buffer, pH 7.0, containing 0.8 mM EDTA, 10 mM NaN_3, 1 mM GSH, and 2.5 nM H_2O_2. After 10 min at 37°C, 0.25 ml of ice-cold 10% TCA was added and the mixture was centrifuged. To 0.25 ml of the supernatant, 1.5 ml of 0.33 mM Na_2HPO_4 and 0.5 ml of 0.6 mM 5,5′-dithiobis-(2-nitrobenzoic acid) were added; absorbance was measured at 420 nm.

In vivo oxidative stress and apoptosis of HSCs

Cirrhosis was induced by 8 weeks of CCl_4 treatment of rats as described previously (Gandhi et al., 1998). Four days after the last CCl_4 administration, control and cirrhotic rats were injected intraperitonealy 50 mg/kg *tert*-butylhydroperoxide (TBHP), which causes liver injury by inducing oxidative stress (Cogger et al., 2004; Hwang et al., 2005; Zwingmann and Bilodeau, 2006). Blood was drawn and the livers were harvested after 6 h, fixed in paraformaldehyde and the sections were stained with TUNEL reagent and anti-desmin antibody to identify apoptotic HSCs (Thirunavukkarasu et al., 2004a).

Statistical analysis

Experiments were performed in triplicates and repeated 2–4 times. Values shown are means ± SD. Statistical significance between the groups was determined by one-way ANOVA followed by a test for linear trend. A P-value of <0.05 was considered statistically significant.

Results

Superoxide causes death of aHSCs but not qHSCs

Although no obvious morphological changes were noted during 24 h treatment of qHSCs with superoxide (Figs. 1A and 2A), aHSCs showed changes indicative of cell death starting at 3 h of superoxide treatment (Figs. 1B and 2B). Viability of aHSCs, but not qHSCs, decreased with increasing superoxide concentration, the effect being statistically significant at 1.5 mU/ml XO (Fig. 2C). Viability of HSCs isolated from the cirrhotic liver also decreased with superoxide treatment suggesting that the results with passaged HSCs are relevant to in vivo activated HSCs (Fig. 2D).

To investigate the mode of superoxide-induced death of aHSCs, DNA damage was characterized by Comet assay as follows: (a) normal cells (round head, no tail); (b) cells with low levels of DNA damage releasing high molecular weight fragments (decreased head size, and tail width not exceeding the head's diameter); (c) cells with highly damaged DNA releasing low molecular weight fragments (well separated diffused tail is wider than the diameter of the bright DNA head); and (d) cells with extensively fragmented DNA (head is not visible and the quickly fading very weak and diffused tail) (Fairbairn et al., 1995). DNA damage of all three types was evident in some qHSCs (Fig. 3A and Table 1), which may have been due to the cell damage during enzymatic digestion as well as changes in temperature (4–37°C) of the isolation procedure. However, there were no obvious alterations in the DNA damage by superoxide treatment (Fig. 3B and Table 1). In contrast, DNA damage was negligible in unstimulated aHSCs, but increased greatly upon superoxide treatment (Fig. 3C,D and Table 1).

The spontaneous DNA damage in qHSCs was associated with their apoptosis that did not change considerably during treatment with superoxide (Fig. 4A). Furthermore flow cytometry and TUNEL labeling assays also demonstrated no significant difference in the level of apoptosis between control and superoxide-challenged qHSCs (Fig. 5). In contrast, as described previously (Thirunavukkarasu et al., 2004a), superoxide caused time-dependent increase in apoptotic aHSCs that was statistically significant even at 3 h (Fig. 4B). We then compared expression/activation of anti-apoptotic (Bcl-xL, Bcl2) and pro-apoptotic (caspase-3, Bax) molecules as well as ERK1/2, JNK and p38 kinases in superoxide-treated cells as alteration in

their relative expression/activation regulates cell survival. Considerable caspase-3 activation was apparent in qHSCs, which decreased time-dependently both in control and superoxide-treated cells at 6, 12, and 24 h (Fig. 6A). qHSCs did not express Bcl-xL and their expression of Bcl2 and Bax did not change during superoxide treatment (Fig. 6A). However, superoxide caused time-dependent increase in caspase-3 activation and decrease in Bcl-xL expression without affecting Bcl2 or Bax expression (Fig. 6B). To further confirm caspase-3 activation, we measured caspase-3-like activity using the fluorescent enzymatic analysis of superoxide-challenged qHSCs and aHSCs. As seen from Figure 6C, significant caspase-3-like activity was observed in unstimulated qHSCs and this did not change upon stimulation with superoxide. In contrast, very low level of activity was present in unstimulated aHSCs, which increased robustly upon superoxide treatment (Fig. 6C).

Superoxide also caused activation of p38 but not ERK1/2 or JNK in aHSCs, and of none of these molecules in qHSCs (Fig. 7A). Next, we used the inhibitors of caspase-3, p38, ERK, and JNK activation to ascertain if they prevent superoxide-induced death of aHSCs. While none of the inhibitors influenced qHSCs, only p38 kinase and caspase-3 inhibitors reversed the death-inducing effect of superoxide on aHSCs (Fig. 7B).

GSH and antioxidant enzymes

GSH content of superoxide-challenged HSCs was determined considering its important role in influencing oxidative damage (Yu, 1994). Superoxide increased GSH (from 18.4 ± 4.7 ng/μg DNA to 28.3 ± 6.5 ng/μg DNA; $P < 0.01$) in qHSCs, but caused small (statistically insignificant) decrease in aHSCs (from 9.6 ± 1.4 ng/μg DNA to 7.6 ± 1.2 ng/μg DNA). Interestingly, the basal GSH concentration was lower in aHSCs than in qHSCs (9.6 ± 1.4 vs. 18.4 ± 4.7 ng/μg DNA; $P < 0.05$). The basal activities of SOD, catalase and GPx, which are integral part of the cellular antioxidant defense mechanism (Yu, 1994), were lower in aHSCs than in qHSCs. While their activities increased in superoxide-challenged qHSCs, no such effect was observed in aHSCs (Table 2).

Effect of retinoic acid (RA)

Since aHSCs do not contain RA, which maintains glutathione in reduced state, we determined the effect of superoxide on viability, GSH content and activities of antioxidant enzymes in aHSCs treated with RA. Incubation of aHSCs with increasing concentrations of 13-*cis*-retinoic acid (0–5 μM) for 5 days ameliorated death-inducing effect of superoxide in a concentration-dependent manner, and consistent with previous reports (Pinzani et al., 1992; Hellemans et al., 2004) reduced their proliferation (Fig. 8A). The latter effect may also be due to the low level of apoptosis caused by RA treatment (Fig. 8B). In fact, RA treatment alone caused caspase-3 and p38-MAPK activation, which were not altered by superoxide; superoxide did not reduce Bcl-xL expression in RA-treated aHSCs (Fig. 8C). Moreover, preincubation of RA-treated aHSCs with DEVD-fmk and SB203580 did not affect their resistance to superoxide-induced death (Fig. 9A).

RA treatment slightly increased GSH content of aHSCs (statistically insignificant) but did not affect the antioxidant enzyme activities except a moderate increase in GPx (Fig. 9B). However, significant increase in the GSH content but not the antioxidant enzyme activities was observed in superoxide-challenged RA-treated aHSCs (Fig. 9B).

LDH activity, an established marker of the loss of cell membrane integrity, was determined in the extracellular medium to examine if superoxide causes necrosis of aHSCs. Superoxide did not cause LDH release from untreated and RA-treated aHSCs at any time up to 24 h during incubation with superoxide.

Effect of in vivo induction of oxidative stress on HSCs

To determine in vivo relevance of the in vitro effects of superoxide on the two HSC phenotypes, control and CCl_4-induced cirrhotic rats were treated with *tert*-butylhydroperoxide, a reliable model of the induction of hepatic oxidative stress (Cogger et al., 2004; Hwang et al., 2005; Zwingmann and Bilodeau, 2006). Liver injury by TBHP was illustrated by increased AST and LDH in control rats from 60 ± 9 to 202 ± 37 IU/L ($P < 0.01$) and 257 ± 19 to 375 ± 59 ($P < 0.05$) IU/L (n = 4 each) respectively and in cirrhotic rats from 2,067 ± 28 to 2,445 ± 245 IU/L ($P < 0.025$) and 2,085 ± 287 to 2,864 ± 663 IU/L ($P < 0.05$) (n = 5 each) respectively. Hepatic architecture was maintained in TBHP-treated control rats but there was mild centrilobular hepatocyte swelling with focal mild mixed lobular inflammation and occasional hepatocyte dropout. Hepatocytes also showed mild reactive changes with mild lobular disarray, but there was no evidence of confluent parenchymal necrosis and significant cholestasis (Fig. 10A). In TBHP-treated cirrhotic rats, hepatic morphological features (Fig. 10B) were similar to that of vehicle-treated rats (not shown) with architectural destruction by nodules of regenerative hepatocytes surrounded by fibrous bands. There was mild mixed inflammation, mild bile ductular proliferation and minimal interface activity. Hepatocytes showed diffuse swelling with moderate mixed macro- and microvesicular steatosis. Scattered hepatocyte apoptosis was noted, with foci of confluent parenchymal acidophilic necrosis. We used TUNEL staining in conjunction with immunohistochemical localization of desmin as both HSC phenotypes express desmin while α-sma is expressed only by aHSCs. By this method, no apoptotic HSCs were found in the livers of vehicle- or TBHP-treated control rats (Fig. 10C,D). Consistent with our previous report (Thirunavukkarasu et al., 2004a), scattered apoptotic HSCs was observed in vehicle-treated cirrhotic liver (Fig. 10E). This increased significantly in the livers of TBHP-treated cirrhotic rats (Fig. 10F) (7 ±2% in untreated versus 35 ± 5% in TBHP-treated; $P < 0.001$).

Discussion

ROS, generated as by-products of cellular metabolism and by specific plasma membrane oxidases, elicit several physiological and pathological effects (Yu, 1994;Pietrangelo, 1996;Li et al., 1997,1999). Moderately increased ROS activate signaling pathways responsible for physiological processes. However, ROS and their lipid peroxidation products can also cause cell death by damaging macromolecules including genomic DNA (Yu, 1994). The qHSCs exhibited significant level of spontaneous apoptosis, which might occur as a result of harsh enzymatic digestion procedure of cell isolation causing membrane damage and also by introduction of serum-free condition. It is also likely that within the heterogeneous population of HSCs (Geerts, 2001), a subpopulation of the cells might be susceptible to the damage easily upon removal from their in vivo environment. Considering this, we expected that spontaneously apoptotic qHSCs would be vulnerable to the damaging actions of superoxide during early culture. However, no additional DNA damage, nuclear condensation and death were apparent in superoxide-treated qHSCs. These results are compatible with the absence of apoptotic qHSCs in the normal liver subjected to oxidative stress in vivo. In contrast, no spontaneous DNA damage or apoptosis was observed in fully activated HSC, but oxidative stress caused their apoptosis both in vitro and in vivo. Superoxide-induced death of aHSCs was predominantly apoptotic as demonstrated by decreased Bcl-xL expression, caspase-3 activation, nuclear condensation, and lack of LDH release.

Increased oxidative stress and decreased GSH, which controls cell's redox state by scavenging ROS and maintaining GPx activity, are associated with apoptotic cell death (Hayes and McLellan, 1999). Previous work has shown that GSH depletion induces apoptosis of hepatocytes (Rauen et al., 1999) and sensitizes them to TNF-α-induced apoptosis (Colell et al., 1998). Moreover, cultured neurons are protected from oxidative stress-induced apoptosis upon

inhibition of GSH depletion (Ahlemeyer and Krieglstein, 2000). These observations and our data suggest that RA provides protection against oxidative stress by maintaining higher GSH levels in qHSCs and RA-treated aHSCs (Yu, 1994). RA, which has immunomodulatory, anti-inflammatory, antiapoptotic and antioxidative properties (Fumarulo et al., 1991; Ahlemeyer and Krieglstein, 2000), inhibits culture-induced activation of HSCs (Chi et al., 2003), and prevents proliferation of aHSCs (Davis et al., 1990; Pinzani et al., 1992; Hellemans et al., 2004). Pinzani et al. (1992) reported that the uptake of exogenously added RA to the culture medium by aHSCs is associated with their phenotypical reversal to a more quiescent form, and therefore RA treatment could be a strategy to reverse fibrosis. In this regard, all-*trans*-RA was shown to ameliorate CCl4-induced fibrosis (Wang et al., 2007). However, it is also important to note that administration of a stable RA analog exacerbated porcine serum-induced hepatic fibrosis in rats (Okuno et al., 1997) These discrepancies might be due to the different isoforms of RA used in these studies, and thus it is difficult to draw a definitive inference about the interactions between RA, ROS and HSCs in vivo with respect to development or reduction of fibrosis. However, it is tempting to suggest that RA might cause reversal of HSC phenotype to non-fibrogenic quiescent form that is resistant to superoxide-induced apoptosis based on our data and those of Davis et al. (1990), Pinzani et al. (1992), Hellemans et al. (2004), and Wang et al. (2007).

Several important mechanisms of eukaryotic cell regulation involve signal transduction via MAPKs (Kyriakis and Avruch, 2001). Our data show that p38-MAPK inhibition reverses superoxide-induced death of aHSCs. In contrast, viability of qHSCs and RA-treated aHSCs was marginally, if at all, affected by superoxide, without or with pretreatment with p38-MAPK inhibitor. Interestingly, RA treatment of aHSCs itself caused caspase-3 and p38 activation and low level of apoptosis. But level of activation of caspase-3 and p38 or apoptosis of RA-treated aHSCs did not increase upon superoxide treatment. Our data do not explain the mechanisms of the activation of caspase-3 and p38 by RA alone or of the prevention of the increase in their activation by RA upon superoxide treatment. It is also not known if the inhibition of proliferation of aHSCs by RA observed before (Pinzani et al., 1992; Hellemans et al., 2004) was associated with some level of apoptosis. Nevertheless, our results suggest that p38-MAPK is an important signaling pathway associated with superoxide-induced apoptosis of aHSCs.

An important difference between the HSC phenotypes was absence of Bcl-xL and lower expression of Bcl2 in qHSCs as compared to aHSCs. Robust increase in Bcl2 expression and decrease in Bax expression were suggested to be a mechanism of the resistance of human HSCs to superoxide (Novo et al., 2006b). However, in rat aHSCs, superoxide treatment did not affect Bcl2 and Bax but caused activation of caspase-3 and reduced Bcl-xL expression. Why qHSCs are resistant to the damaging effects of superoxide in the absence of Bcl-xL, lower Bcl2 and high Bax expression warrants further investigation.

Several studies have shown concentration-dependent variability in the effects of ROS on aHSCs. Human portal myofibroblasts (fibulin-2 and α-sma-positive), which are similar to aHSCs (α-sma-positive), undergo apoptosis upon treatment with H_2O_2 and following 15-d-PGJ_2-induced intracellular oxidative stress (Li et al., 2001). Similarly, increased oxidative stress is a mechanism of gliotoxin-induced apoptosis and secondary necrosis of human aHSCs (Kweon et al., 2003). The pro-oxidant molecule 3,4-methylenedioxymethamphetamine also caused apoptosis of aHSC cell line CFC-2G (Montiel-Duarte et al., 2004). In our previous (Thirunavukkarasu et al., 2004a) and this investigation, we observed apoptosis of rat aHSCs by superoxide generated from 1 mM hypoxanthine and 2 mU/ml oxanthine oxidase. However, superoxide generated from concentrations of hypoxanthine and oxanthine oxidase similar to that used here did not cause apoptosis of human aHSCs, but strongly inhibited their PDGF-induced proliferation (Galli et al., 2005; Novo et al., 2006a). Interestingly, rapid bursts of higher concentrations of superoxide caused apoptosis of human aHSCs (Galli et al., 2005), but also

stimulated fibrogenic activity in the remaining cells (Casini et al., 1997). Together, these results and those reported by Novo et al. (2006a) suggest that the susceptibility of rodent and human aHSCs to superoxide-induced damage may be different, and related to differential Bax, Bcl2, and Bcl-xL expression (Novo et al., 2006b). Moreover, even though human aHSCs undergo apoptosis at higher superoxide concentration (Novo et al., 2006a), a subpopulation of these cells may be resistant to such effect and retains ability to produce fibrogenic response (Casini et al., 1997). The existence of heterogeneous cell populations is also apparent in fully activated HSCs. Although these cells are suggested to be highly resistant to apoptosis, a subpopulation appears to be sensitive to proapoptotic stimuli as indicated by the presence of apoptotic aHSCs in the actively fibrotic liver (Thirunavukkarasu et al., 2004a; Fig. 10E). Furthermore, rapid removal of aHSCs during resolution of liver fibrosis (Iredale et al., 1998; Thirunavukkarasu et al., 2004b) indicates their vulnerability to apoptotic stimuli. ROS produced physiologically are beneficial for the normal cellular metabolism and function. However, their increased production in inflammatory conditions, such as in the injured liver, can be damaging to various cell types. Our in vitro and in vivo results thus suggest that superoxide-induced apoptosis of aHSCs might be an important mechanism in limiting ongoing fibrosis.

In summary, inability of superoxide to stimulate caspase-3 and p38-MAPK activation in qHSCs (presumably due to RA) renders them resistant to its pro-death effect. The concentration of superoxide that causes apoptosis/necrosis of human aHSCs (Novo et al., 2006a) is higher than that used in our study with rat aHSCs. A more comprehensive examination of the interspecies differences as well as heterogeneity in the sensitivity of aHSCs to ROS will provide better understanding of clinical relevance of these findings.

Abbreviations

aHSCs	activated hepatic stellate cells
GPx	glutathione peroxidase
GSH	glutathione
HX	hypoxanthine
qHSCs	quiescent hepatic stellate cells
ROS	reactive oxygen species
SOD	superoxide dismutase
XO	xanthine oxidase

Acknowledgments

We thank Ms. Holly Grunebach, Mr. Mark Ross, Mr. Sean Alber and Mr. Adam Kichler for excellent technical assistance. This work was supported by VA Merit award (CRG), and NIH grants DK 54411(CRG), DK37320 and DK56621 (SLF) and CA102325 and CA106280 (TW).

Contract grant sponsor: VA Merit award.

Contract grant sponsor: NIH;

Contract grant numbers: DK 54411, DK37320, DK56621, CA102325, CA106280.

Literature Cited

Ahlemeyer B, Krieglstein J. Inhibition of glutathione depletion by retinoic acid and tocopherol protects cultured neurons from staurosporine-induced oxidative stress and apoptosis. Neurochem Int 2000;36:1–5. [PubMed: 10566953]

Casini A, Ceni E, Salzano R, Biondi P, Parola M, Galli A, Foschi M, Caligiuri A, Pinzani M, Surrenti C. Neutrophil-derived superoxide anion induces lipid peroxidation and stimulates collagen synthesis in human hepatic stellate cells: Role of nitric oxide. Hepatology 1997;25:361–367. [PubMed: 9021948]

Chi X, Anselmi A, Watkins S, Gandhi CR. Prevention of cultured stellate cell transformation and endothelin-B receptor up-regulation by retinoic acid. Br J Pharmacol 2003;139:765–774. [PubMed: 12813000]

Choi SS, Sicklick JK, Ma Q, Yang L, Huang J, Qi Y, Chen W, Li YX, Goldschmidt-Clermont PJ, Diehl AM. Sustained activation of Rac1 in hepatic stellate cells promotes liver injury and fibrosis in mice. Hepatology 2006;44:1267–1277. [PubMed: 17058265]

Cogger VC, Muller M, Fraser R, McLean AJ, Khan J, Le Couteur DG. The effects of oxidative stress on the liver sieve. J Hepatol 2004;41:370–376. [PubMed: 15336438]

Colell A, García-Ruiz C, Miranda M, Ardite E, Marí M, Morales A, Corrales F, Kaplowitz N, Fernández-Checa JC. Selective glutathione depletion of mitochondria by ethanol sensitizes hepatocytes to tumor necrosis factor. Gastroenterology 1998;115:1541–1551. [PubMed: 9834283]

Davis BH, Kramer RT, Davidson NO. Retinoic acid modulates rat Ito cell proliferation, collagen, and transforming growth factor beta production. J Clin Invest 1990;86:2062–2070. [PubMed: 2254460]

Fairbairn DW, Olive PL, O'Neill KL. The comet assay: A comprehensive review. Mutat Res 1995;339:37–59. [PubMed: 7877644]

Friedman SL. Molecular regulation of hepatic fibrosis, an integrated cellular response to tissue injury. J Biol Chem 2000;275:2247–2250. [PubMed: 10644669]

Fumarulo R, Conese M, Riccardi S, Giordano D, Montemurro P, Colucci M, Semeraro N. Retinoids inhibit the respiratory burst and degranulation of stimulated human polymorphonuclear leukocytes. Agents Actions 1991 1991;34:339–342.

Galli A, Svegliati-Baroni G, Ceni E, Milani S, Ridolfi F, Salzano R, Tarocchi M, Grappone C, Pellegrini G, Benedetti A, Surrenti C, Casini A. Oxidative stress stimulates proliferation and invasiveness of hepatic stellate cells via a MMP2-mediated mechanism. Hepatology 2005;41:1074–1084. [PubMed: 15841469]

Gandhi CR, Nemoto EM, Watkins SC, Subbotin VM. An endothelin receptor antagonist TAK-044 ameliorates carbon tetrachloride-induced acute liver injury and portal hypertension in rats. Liver 1998;18:39–48. [PubMed: 9548266]

Geerts A. History, heterogeneity, developmental biology, and functions of quiescent hepatic stellate cells. Semin Liver Dis 2001;21:311–335. [PubMed: 11586463]

Geerts, A.; DeBleser, P.; Hautekeete, ML.; Niki, T.; Wisse, E. Fat-storing, (Ito) cell biology. In: Arias, IM.; Boyer, JL.; Fasuto, N.; Jakoby, WB.; Schachter, DL.; Shafritz, DA., editors. The liver: Biology and pathobiology. New York: Raven Press, Ltd.; 1994. p. 819-838.

Hayes JD, McLellan LI. Glutathione and glutathione-dependent enzymes represent a co-ordinately regulated defence against oxidative stress. Free Rad Res 1999;31:273–300.

Hellemans K, Verbuyst P, Quartier E, Schuit F, Rombouts K, Chandraratna RA, Schuppan D, Geerts A. Differential modulation of rat hepatic stellate phenotype by natural and synthetic retinoids. Hepatology 2004;39:97–108. [PubMed: 14752828]

Helma C, Uhl MA. Domain image-analysis program for the single-cell gel-electrophoresis (comet) assay. Mutat Res 2000;466:9–15. [PubMed: 10751720]

Hwang JM, Wang CJ, Chou FP, Tseng TH, Hsieh YS, Hsu JD, Chu CY. Protective effect of baicalin on tert-butyl hydroperoxide-induced rat hepatotoxicity. Arch Toxicol 2005;79:102–109. [PubMed: 15645217]

Iredale JP, Benyon RC, Pickering J, McCullen M, Orthrop M, Pawley S, Hovell C, Arthur MJ. Mechanisms of spontaneous resolution of rat liver fibrosis. Hepatic stellate cell apoptosis and reduced hepatic expression of metalloproteinase inhibitors. J Clin Invest 1998;102:538–549. [PubMed: 9691091]

Klebanoff, SL. Inflammation: Basic princliples and clinical correlates. Gallin, JI.; Goldstein, IM.; Snyderman, I., editors. New York: Raven Press; 1988. p. 391-444.

Knight TR, Ho YS, Farhood A, Jaeschke H. Peroxynitrite is a critical mediator of acetaminophen hepatotoxicity in murine livers: Protection by glutathione. J Pharmacol Exp Ther 2002;303:468–475. [PubMed: 12388625]

Kweon YO, Paik YH, Schnabl B, Qian T, Lemasters JJ, Brenner DA. Gliotoxin-mediated apoptosis of activated human hepatic stellate cells. J Hepatol 2003;39:38–46. [PubMed: 12821042]

Kyriakis JM, Avruch J. Mammalian mitogen-activated protein kinase signal transduction pathways activated by stress and inflammation. Physiol Rev 2001;81:807–869. [PubMed: 11274345]

Lee KS, Buck S, Houglum K, Chojkier M. Activation of hepatic stellate cells by TGF α and collagen type I is mediated by oxidative stress through c-myb expression. J Clin Invest 1995;96:2461–2468. [PubMed: 7593635]

Li P-F, Dietz R, von Harsdorf R. Differential effect of hydrogen peroxide and superoxide anion on apoptosis and proliferation of vascular smooth muscle cells. Circulation 1997;96:3602–3609. [PubMed: 9396461]

Li P-F, Dietz R, von Harsdorf R. Superoxide induces apoptosis in cardiomyocytes, but proliferation and expression of transforming growth factor-b1 in cardiac fibroblasts. FEBS Lett 1999;448:206–210. [PubMed: 10218477]

Li L, Tao J, Davaille J, Feral C, Mallat A, Rieusset J, Vidal H, Lotersztajn S. 15-deoxy-Delta 12,14-prostaglandin J2 induces apoptosis of human hepatic myofibroblasts. A pathway involving oxidative stress independently of peroxisome-proliferator-activated receptors. J Biol Chem 2001;276:38152–38158. [PubMed: 11477100]

Montiel-Duarte C, Ansorena E, Lopez-Zabalza MJ, Cenarruzabeitia E, Iraburu MJ. Role of reactive oxygen species, glutathione and NF-kappaB in apoptosis induced by 3,4-methylenedioxymethamphetamine ("Ecstasy") on hepatic stellate cells. Biochem Pharmacol 2004;67:1025–1033. [PubMed: 15006539]

Novo E, Marra F, Zamara E, Valfrè di Bonzo L, Caligiuri A, Cannito S, Antonaci C, Colombatto S, Pinzani M, Parola M. Dose-dependent and divergent effects of superoxide anion on cell death, proliferation and migration of activated human hepatic stellate cells. Gut 2006a;55:90–97. [PubMed: 16041064]

Novo E, Marra F, Zamara E, Valfrè di Bonzo L, Monitillo L, Cannito S, Petrai I, Mazzocca A, Bonacchi A, De Franco RS, Colombatto S, Autelli R, Pinzani M, Parola M. Overexpression of Bcl-2 by activated human hepatic stellate cells: Resistance to apoptosis as a mechanism of progressive hepatic fibrogenesis in humans. Gut 2006b;55:1174–1182. [PubMed: 16423888]

Okuno M, Moriwaki H, Imai S, Muto Y, Kawada N, Suzuki Y, Kojima S. Retinoids exacerbate rat liver fibrosis by inducing the activation of latent TGF-beta in liver stellate cells. Hepatology 1997;26:913–921. [PubMed: 9328313]

Parola M, Pinzani M, Casini A, Albano E, Poli G, Gentilini A, Gentilini P, Dianzani MU. Stimulation of lipid peroxidation or 4-hydroxynonenal treatment increases procollagen alpha 1 (I) gene expression in human liver fat-storing cells. Biochem Biophys Res Commun 1993;194:1044–1050. [PubMed: 8352762]

Pietrangelo A. Metals, oxidative stress and hepatic fibrosis. Sem Liver Dis 1996;16:13–30.

Pinzani M, Gentilini P, Abboud HE. Phenotypical modulation of liver fat-storing cells by retinoids. Influence on unstimulated and growth factor-induced cell proliferation. J Hepatol 1992;14:211–220. [PubMed: 1500685]

Rauen U, Reuters I, Fuchs A, de Groot H. Oxygen-free radical-mediated injury to cultured rat hepatocytes during cold incubation in preservation solutions. Hepatology 1997;26:351–357. [PubMed: 9252145]

Rauen U, Polzar B, Stephan H, Mannherz HG, De Groot D. Cold-induced apoptosis in cultured hepatocytes and liver endothelial cells: Mediation by reactive oxygen species. FASEB J 1999;13:155–168. [PubMed: 9872940]

Svegliati, Baroni G.; D'Ambrosio, L.; Ferretti, G.; Casini, A.; Di Sario, A.; Salzano, R.; Ridolfi, F.; Saccomanno, S.; Jezequel, AM.; Benedetti, A. Fibrogenic effect of oxidative stress on rat hepatic stellate cells. Hepatology 1998;27:720–726. [PubMed: 9500700]

Thirunavukkarasu C, Watkins S, Harvey SAK, Gandhi CR. Superoxide-induced apoptosis of activated rat hepatic stellate cells. J Hepatol 2004a;41:567–575. [PubMed: 15464236]

Thirunavukkarasu C, Yang Y, Subbotin VM, Harvey SAK, Fung J, Gandhi CR. Endothelin receptor antagonist TAK-044 arrests and reverses the development of carbon tetrachloride-induced cirrhosis in rats. Gut 2004b;53:1010–1019. [PubMed: 15194653]

Thirunavukkarasu C, Uemura T, Wang LF, Watkins SC, Gandhi CR. Normal rat hepatic stellate cells respond to endotoxin in LBP-independent manner to produce inhibitor(s) of DNA synthesis in hepatocytes. J Cell Physiol 2005;204:654–665. [PubMed: 15828022]

Wang L, Potter JJ, Rennie-Tankersley L, Novitskiy G, Sipes J, Mezey E. Effects of retinoic acid on the development of liver fibrosis produced by carbon tetrachloride in mice. Biochim Biophys Acta 2007;1772:66–71. [PubMed: 17011172]

Yu BP. Cellular defenses against damage from reactive oxygen species. Pharmacol Rev 1994 1994;74:139–162.

Zwingmann C, Bilodeau M. Metabolic insights into the hepatoprotective role of N-acetylcysteine in mouse liver. Hepatology 2006;43:454–463. [PubMed: 16496303]

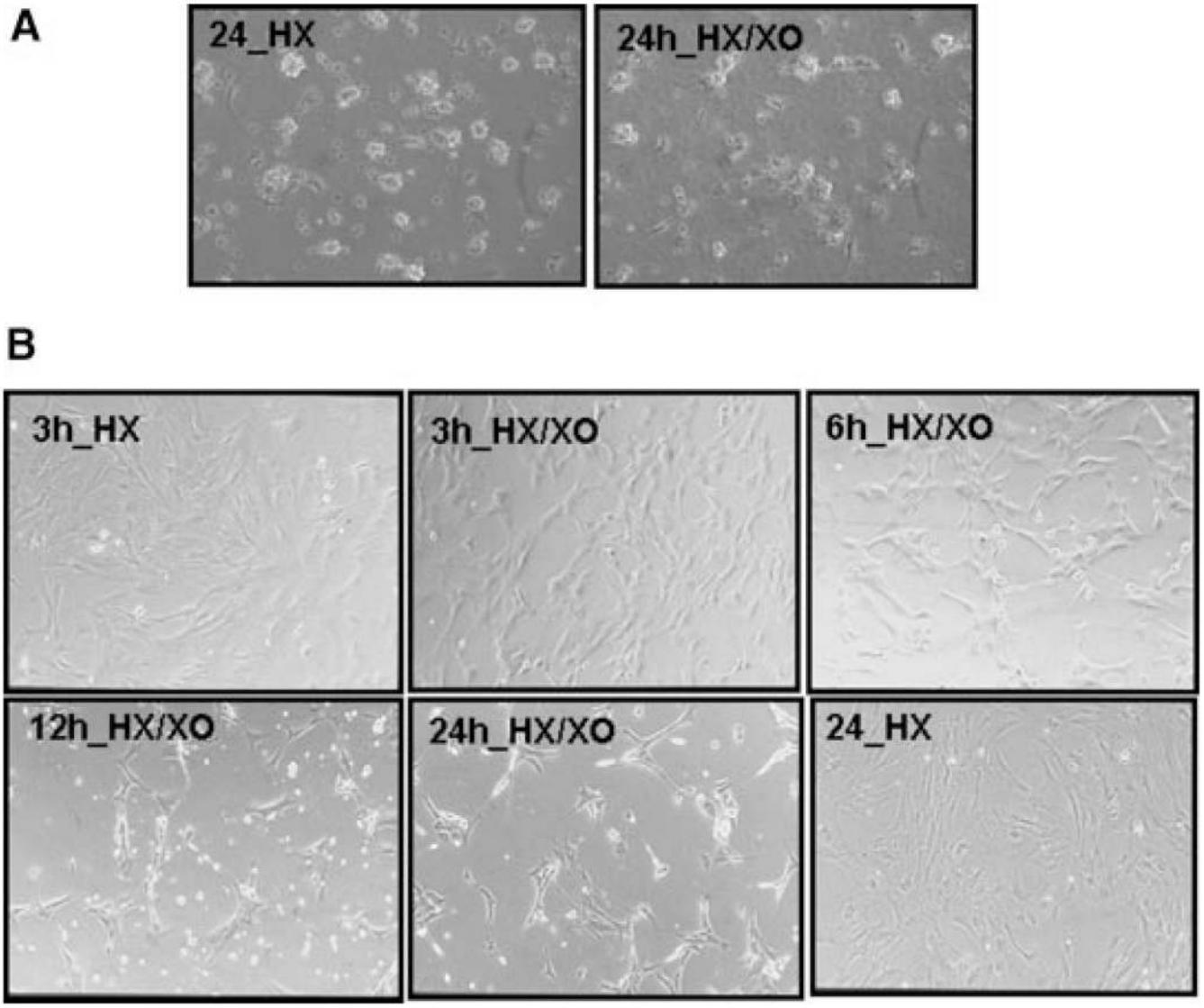

Fig. 1.

Morphological changes in qHSCs and aHSCs during superoxide treatment. A: Phase contrast photo micrographs of qHSCs (A)and aHSCs (B) treated with 1 mMH ± 2 mU/mlXO for indicated times show no effect on the morphology of qHSCs but progressive detachment and death of aHSCs starting at 3 h. Magnification 200×.

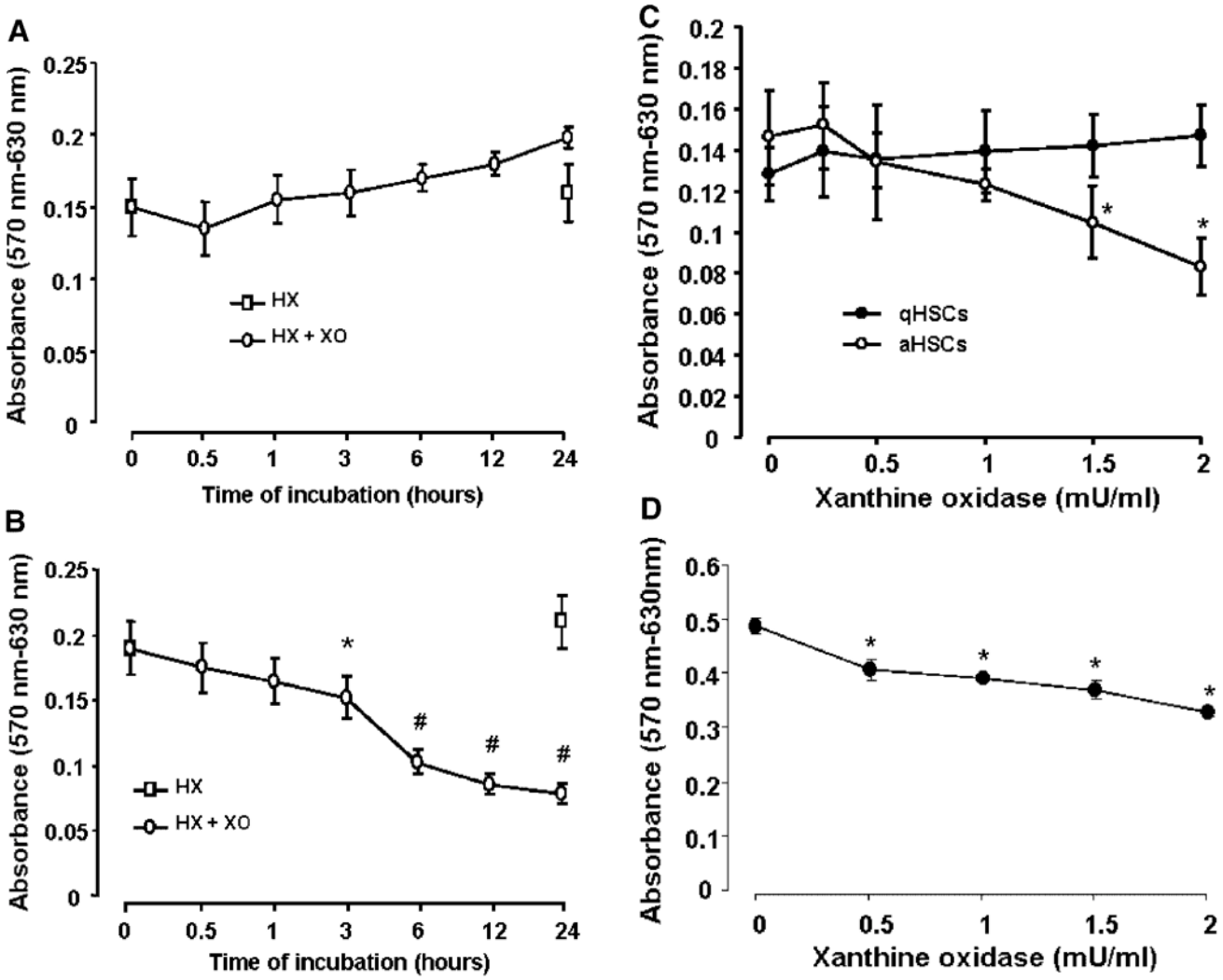

Fig. 2.

Time-course of superoxide-induced change in viability. A:qHSCsor(B)aHSCs were in cubated with 1 mMHX ± 2 mU/ml XO for indicated time period or(C)for 24h with 1 mMHX and indicated concentrations of XO in serum-free DMEM.D:HSCs isolated from CC14-cirrhoticliver were subjected to superoxide treatment on day 2. Viability, determined by MTT assay show death of HSCs activated both in vitro (B,C) and in vivo (D). *P<0.05 versus "0"; #P<0.001 versus "0".

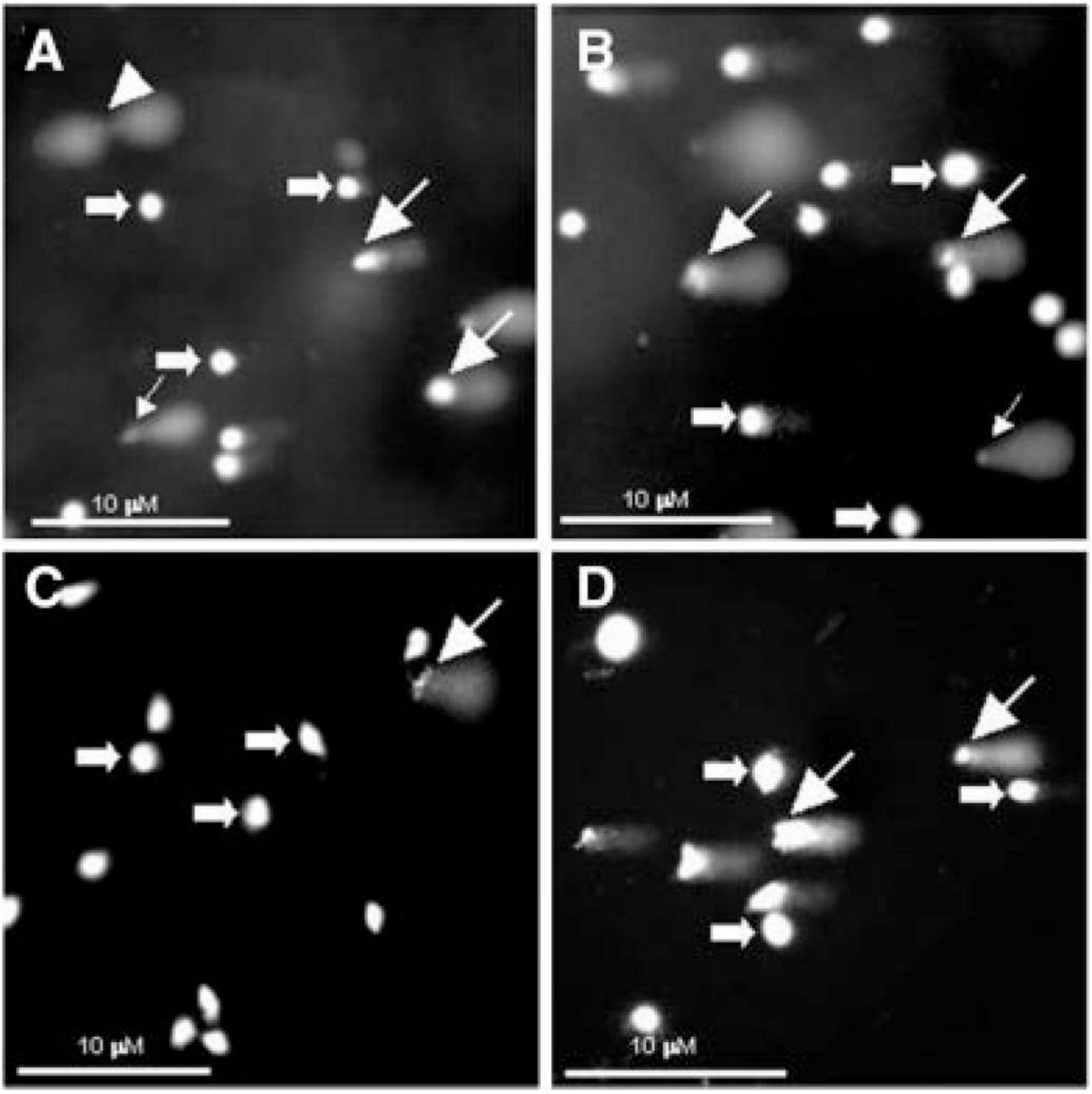

Fig. 3.

Effect of superoxide on DNA damage. A,B: qHSCs or (C,D) aHSCs were incubated with 1 mM HX in the absence (A,C) or presence (B,D) of 2 mU/ml XO for 24 h. DNA damage was determined by comet assay. Thick arrows (normal cells); thin arrows with large heads (high molecular weight DNA fragments); thin arrows with small heads (low molecular weight DNA fragments); arrowheads (intermediate molecular weight DNA fragments). Note that there is no significant change in the spontaneous DNA damage of qHSCs by superoxide, but the treatment induced strong DNA damage in aHSCs that was minimal under basal condition.

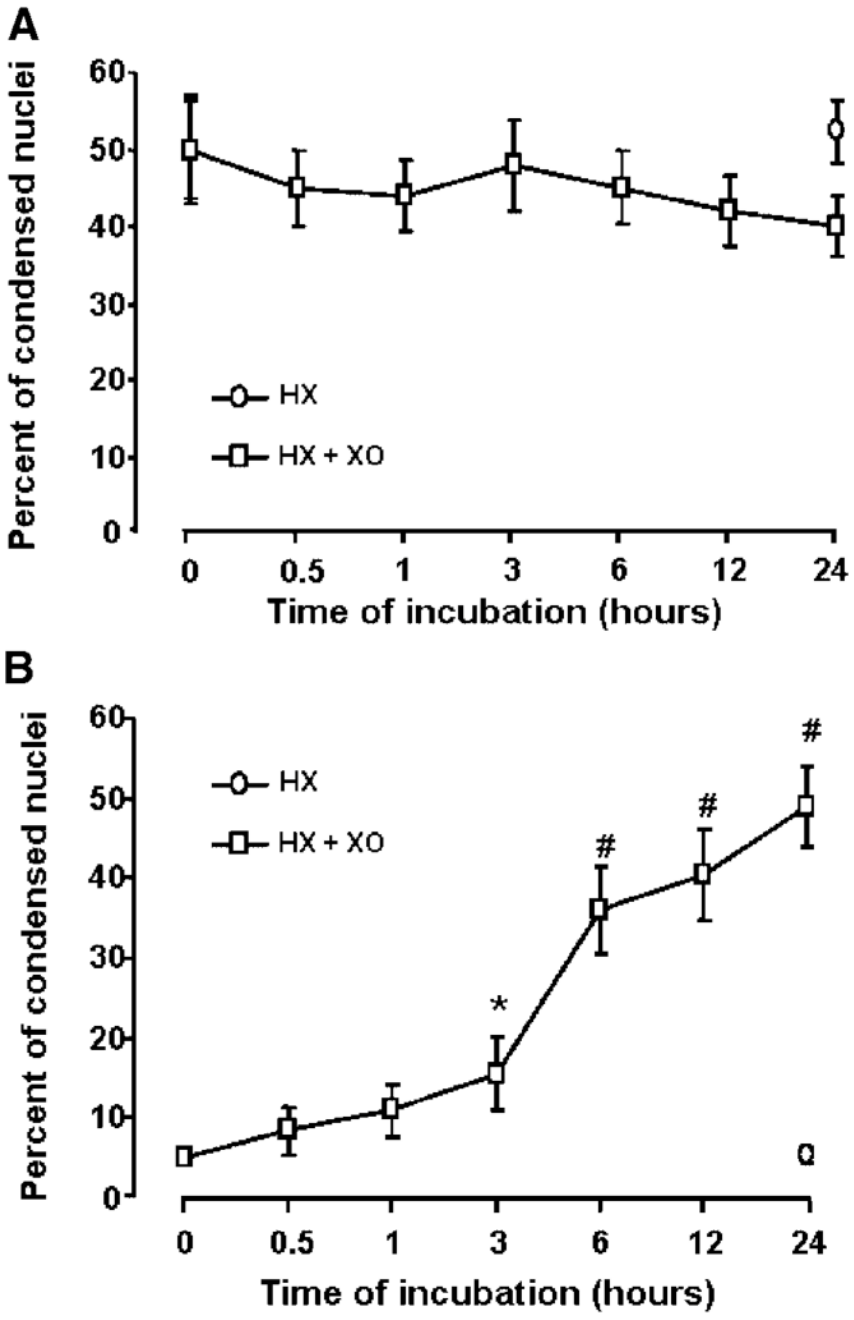

Fig. 4.

Effect of superoxide on nuclear condensation in HSCs. A:qHSCs or (B) aHSCs were incubated with 1 mMHX ± 2 mU/ml XO for indicated times. Apoptosis was identified by condensed nuclei after staining with Hoechst reagent. Ten fields per slide (each in triplicate) were counted for condensed nuclei. *P<0.05 versus "0"; $^{\#}P$<0.001 versus "0".

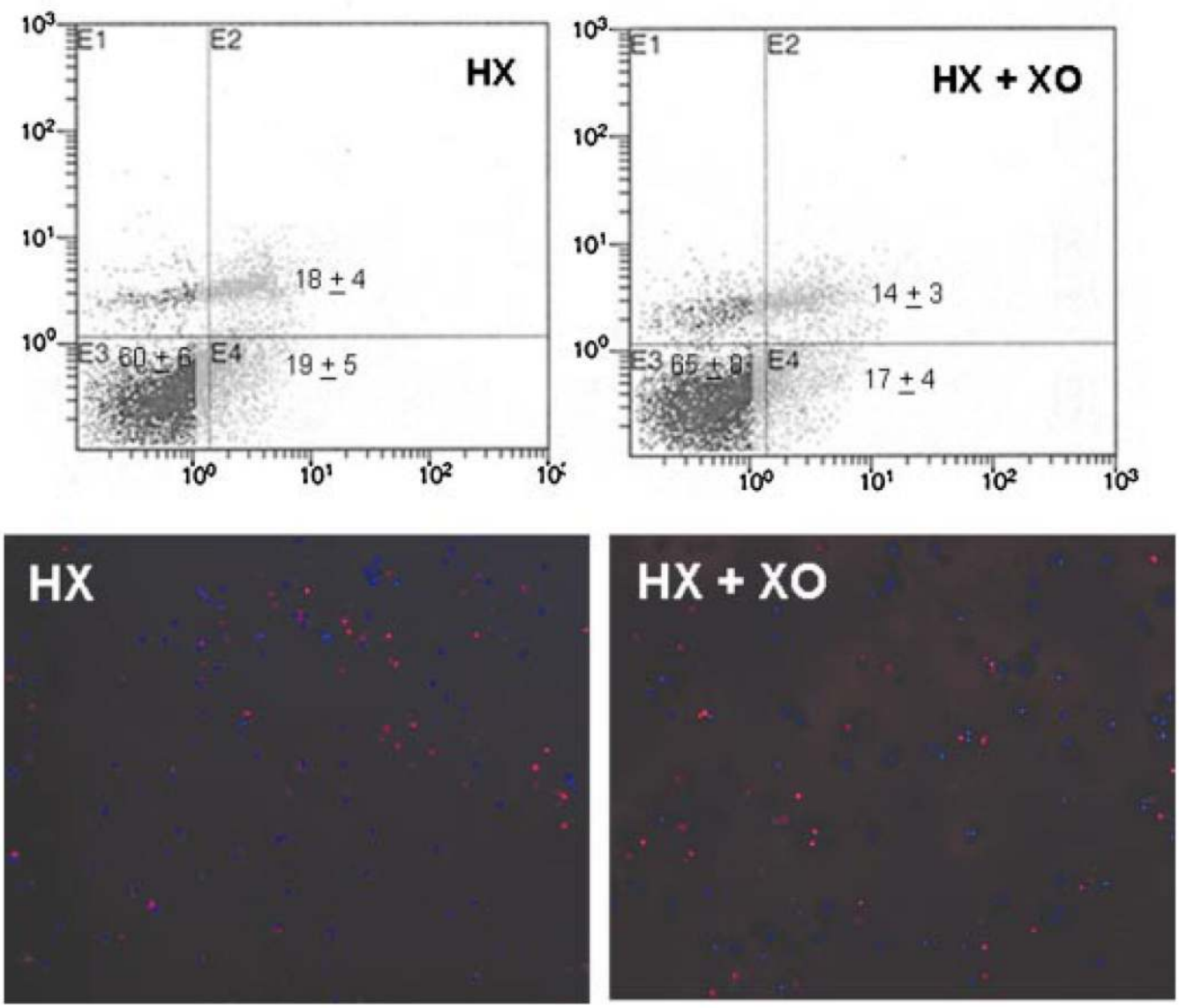

Fig. 5.

Apoptosis via flow cytometry and TUNEL labeling of qHSCs without and with superoxide challenge. A: The cells were stained with annexin-Vcy3 and 7-AAD following 24 h incubation with 1 mM hypoxanthine (HX) ± 2 mU/ml xanthine oxidase (XO), and flow cytometry was performed as described in Experimental Procedures. Normal cells (annexin-Vcy3- and 7-AAD-negative, E3); cells in early apoptosis (annexin-Vcy3-positive and 7-AAD-negative, E4); and cells in late apoptosis/necrosis (annexin-Vcy3- and 7-AAD-positive, E2). The values represent number of cells (%) in the specified phase ± SD.B: TUNEL assay was performed on the qHSCs treated with 1 mM HX± 2mU/mlXOfor 24 h as described in Experimental Procedures. A representative experiment performed in duplicates (two repeats) shows apoptotic nuclei (red). Note that there is no significant difference in the level of apoptosis between the control and superoxide-treated cells. [Color figure can be viewed in the online issue, which is available at www.interscience.wiley.com.]

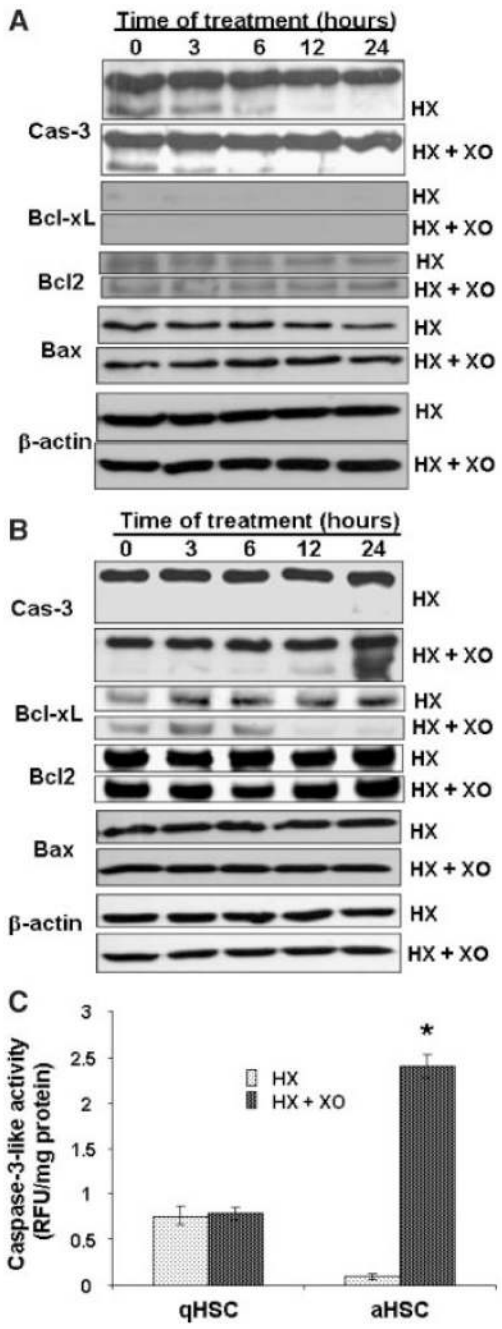

Fig. 6.

Apoptosis-related signaling molecules in superoxide-treated HSCs.A: qHSCs or(B)aHSCs were treated with 1 m MHX ± 2 mU/ml XO for indicated times. Pro- and active forms of caspase-3, and expression of Bcl2, Bcl-xL, and Bax were determined by Western blot analysis. Expression of β-actin is shown to ensure equal loading. C: The cells were treated for 12 h with 1 m Mhypoxanthine ± 2 mU/ml xanthine oxidase. Caspase-3 activity was measured using caspase fluorescent assay kit (BD Biosciences Clontech). **P*<0.001 versus control.

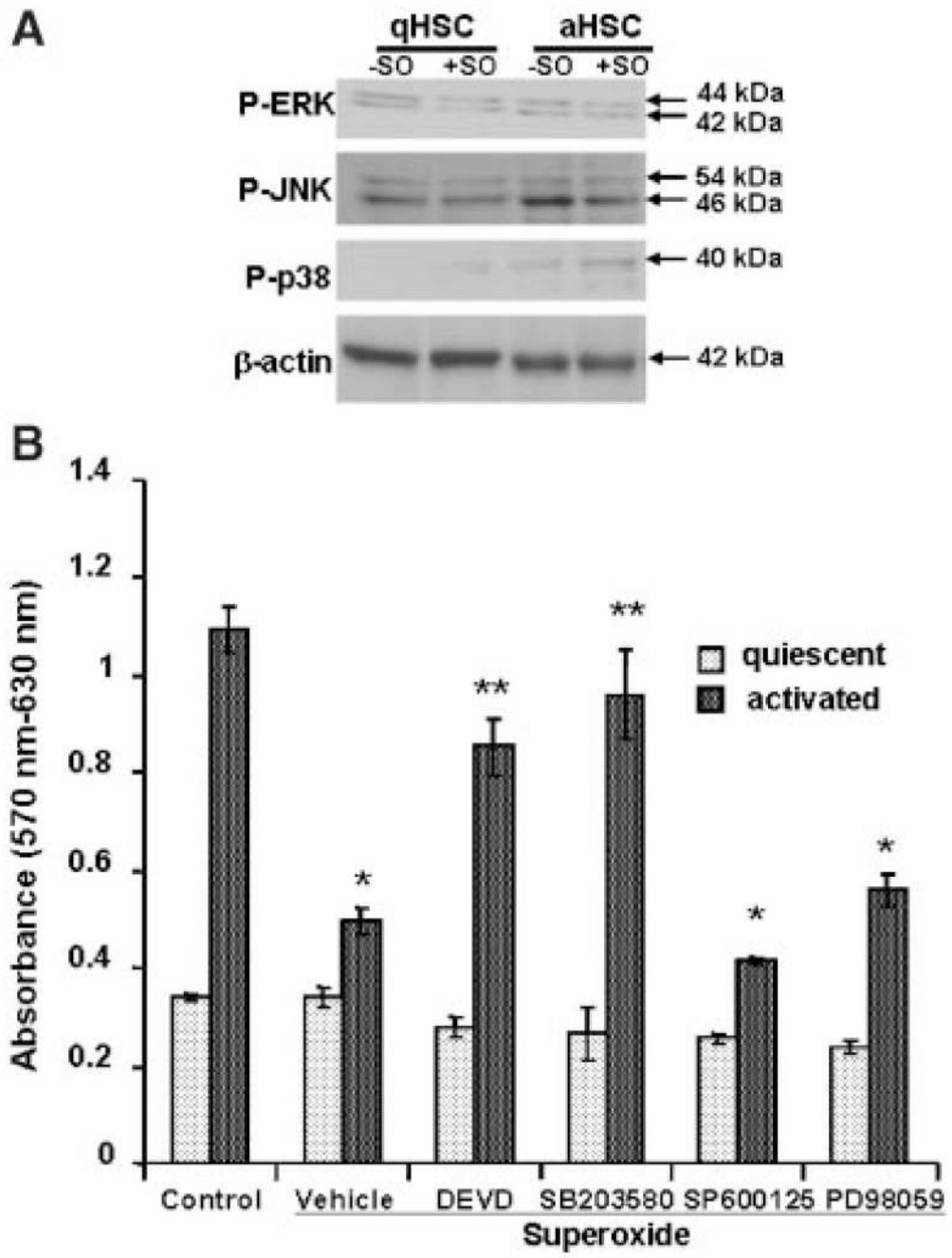

Fig. 7.

A: Effect of superoxide on activation of MAPKs. qHSCs or aHSCs were treated with superoxide for 3 h, and the lysates (20 μg protein) were subjected to SDS–PAGE followed by immunoblotting with antibodies against P-ERK, P-JNK, and P-p38. Equal loading was ensured by β-actin expression. B: Effect of pretreatment with caspase-3 and MAPK inhibitors on viability of HSCs incubated with superoxide. qHSCs or aHSCs were incubated with inhibitors of the activation of caspase-3 (DEVD-fmk), p38 (SB203580), JNK (SP600125), or ERK1/2 (PD98059) (all at 10 μM concentration) for 30 min prior to the addition of 1 mM HX ± 2 mU/ml XO. MTT assay was performed at 24 h. **P*<0.01 versus control; ***P*<0.05 versus control and superoxide.

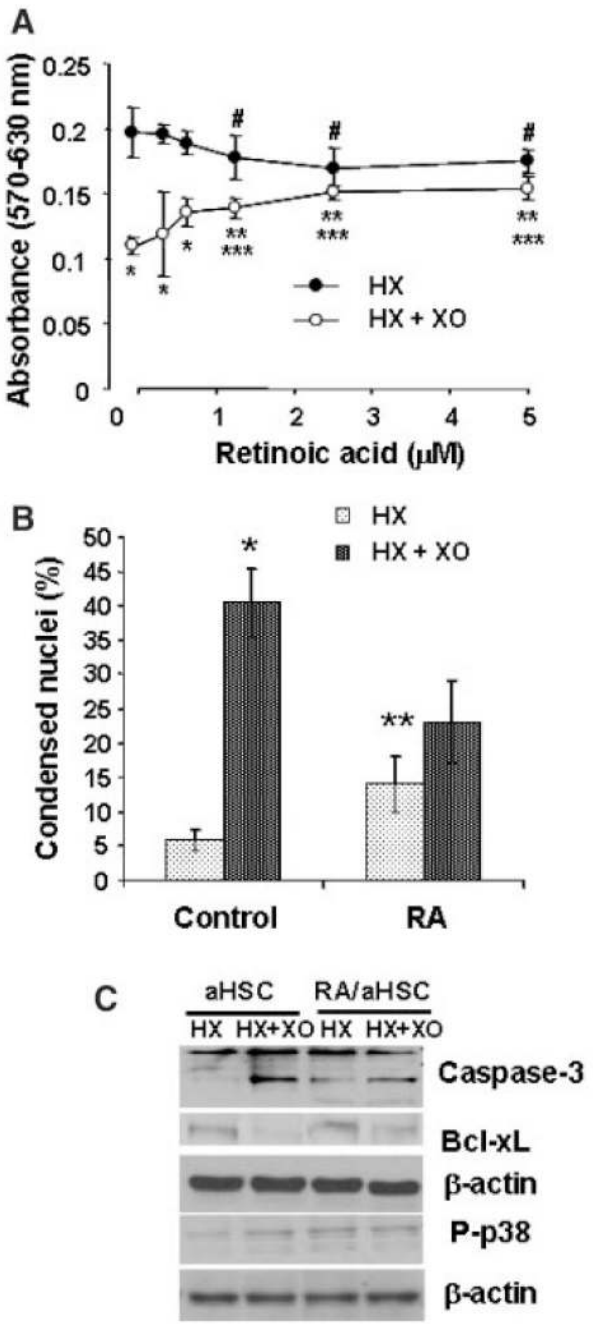

Fig. 8.

Effect of RA on superoxide-induced changes in viability (A) nuclear condensation (B), and Bcl-xL, caspase-3 and p38-MAPK (C) of aHSCs. Cells were incubated in the absence (0 or Control) or presence of 0.3–5.0 μM 13-*cis*-RA for 5 days, washed and placed in serum-free medium without (0 or Control) or with RA, and challenged with 1 mM HX ± 2 mU/ml XO. In (B,C), cells were incubated with 2.5 μM RA for 5 days. Various determinations were made at 24 h except p38-MAPK (3 h). A: **P*<0.005 versus HX; ***P*<0.05 versus HX; ****P*<0.05 versus "0" RA and HX + XO; #*P*< 0.05 versus "0" RA. B: **P*< 0.005 versus HX; ***P*<0.05 versus Control.

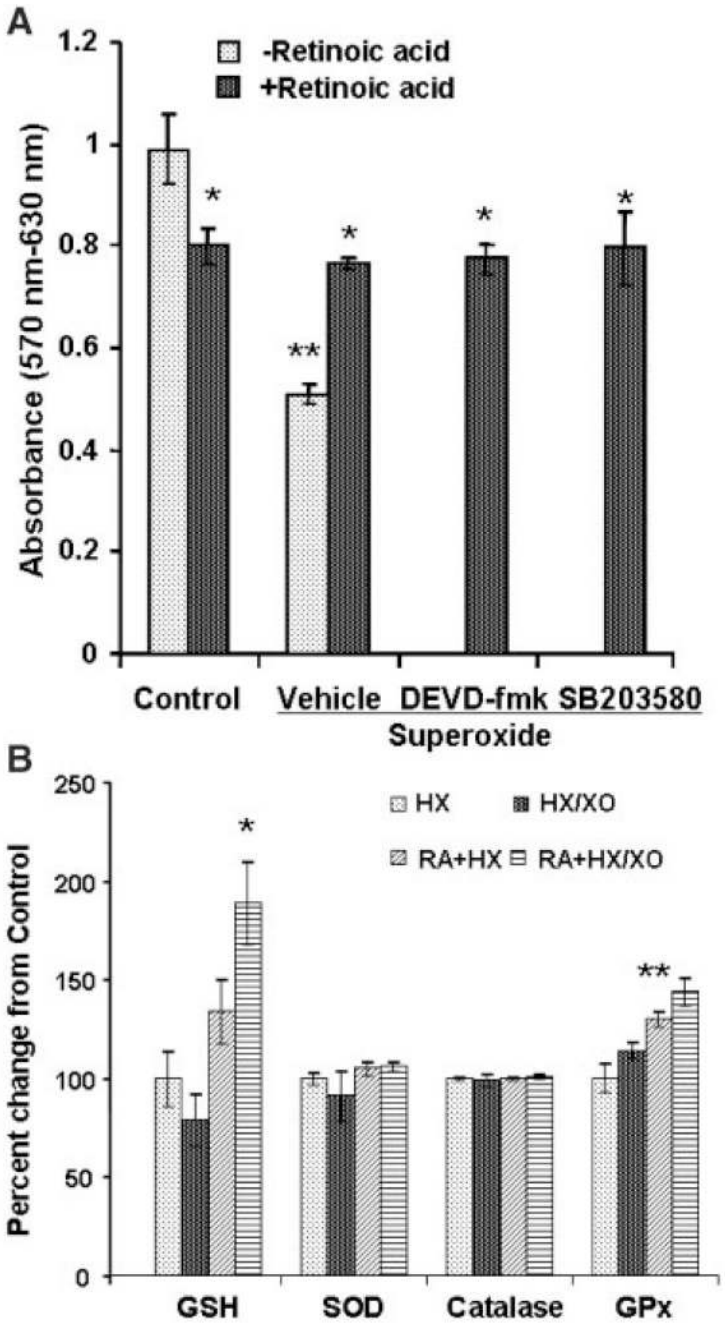

Fig. 9.

A: Effect of pretreatment with caspase-3 and p38-MAPK inhibitors on superoxide-induced death of RA-treated aHSCs. aHSCs were incubated in the presence of 2.5 μM 13-*cis*-RA for 5 days, washed and incubated with 10 μM DEVD-fmk or SB203580 for 30 min prior to the addition of 1 mM HX (Control) ± 2 mU/ml XO (Superoxide). MTT assay was performed at 24 h. **P*< 0.05 versus RA; ***P*<0.01 versus control. B: Effect of RA on superoxide-induced changes in GSH and antioxidant enzymes in aHSCs. aHSCs were incubated in the presence of 2.5 μM 13-*cis*-RA for 5 days, washed and stimulated with 1 mM HX ± 2 mU/ml XO for 24 h, after which various assays were performed.**P*<0.05 versus RA+HX and <0.001 versus HX;***P*<0.01 versus HX.

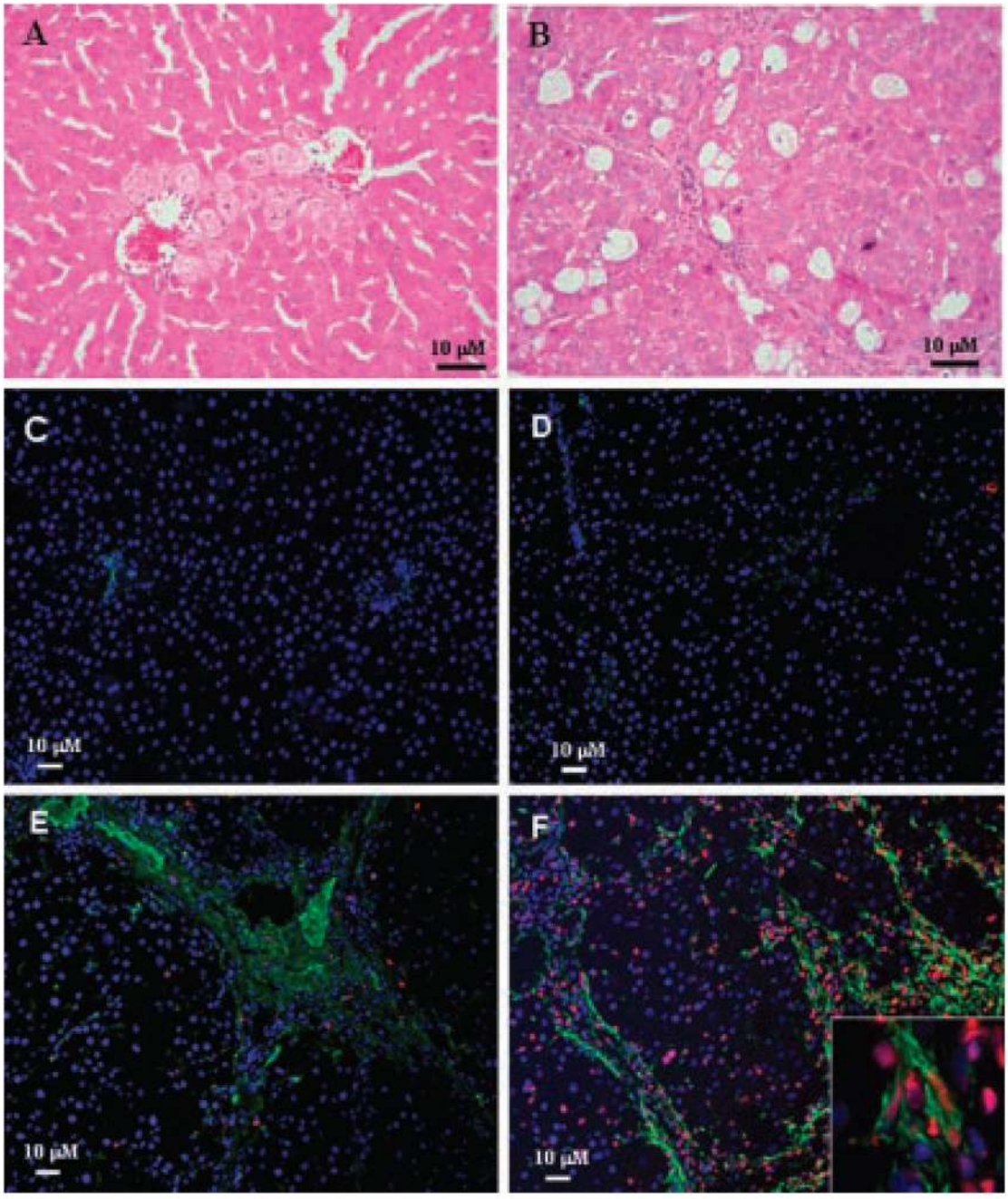

Fig. 10.

Effect of TBHP-induced oxidative stress on HSCs in control and fibrotic rats. CCl4-induced cirrhotic rats or the paired control rats were injected vehicle or TBHP, and at 6 h, the livers were harvested for histopathology and immunohistochemical examination. A,B: Hematoxilyn and Eosin stained sections of livers from TBHP-treated control (A) and cirrhotic (B) rats. C–F: Apoptotic HSCs as determined by desmin (green) and TUNEL (red) co-staining in normal (C,D) and cirrhotic (E,F) livers of vehicle- (C,E) and TBHP- (D,F) treated rats. Photomicrographs are representative of 4 control (vehicle or TBHP-treated) and 5 cirrhotic (vehicle or BHP-treated) rat livers. Inset shows apoptotic aHSCs at higher magnification (400 ×).

TABLE 1

Quantification of DNA damage parameters in superoxide-treated HSCs

	DNA damage		
	Tail length (μm)	**% DNA in tail**	**Tail moment (μm)**
qHSCs			
Control	28.3 ± 6.0	42.9 ± 5.7	18.1 ± 5.2
Superoxide	35.3 ± 4.3	45.9 ± 6.8	17.6 ± 4.4
aHSCs			
Control	6.7 ± 1.1	2.5 ± 1.1	3.8 ± 1.2
Superoxide	32.0 ± 3.3*	50.2 ± 5.8*	19.6 ± 4.0*

The cells were incubated with 1 mM hypoxanthine (Control) or with hypoxanthine and 2 mU/ ml xanthine oxidase (Superoxide) for 24 h. Comet assay was performed to assess DNA damage parameters.

*P<0.001 versus control.

TABLE 2

Effect of superoxide on superoxide dismutase, catalase and glutathione peroxidase

	Hypoxanthine	Hypoxanthine + Xanthine oxidase
qHSCs		
SOD	0.5 ± 0.1	1.3 ± 0.1*
Catalase	1.6 ± 0.2	2.3 ± 0.3*
GPx	62.5 ± 7.5	72.5 ± 6.9**
aHSCs		
SOD	0.25 ± 0.04	0.21 ± 0.05
Catalase	1.3 ± 0.3	0.9 ± 0.1
GPx	38.6 ± 5.2	26.5 ± 3.0*

Enzyme activities were measured in cells incubated with 1 mM HX±2.0 mU/ml of XO for 24 h. Activities are expressed as follows: SOD, Units/mg protein (one enzyme unit corresponds to the amount of enzyme required to cause 50% inhibition of pyrogallol auto-oxidation); catalase, μmol of H_2O_2 consumed/min/mg protein; and GPx, μg of glutathione utilized/min/mg protein.

*$P<0.05$ and

**$P<0.01$ versus respective controls.